

# The Orientation Effect on Superfluid $^3\text{He}$ in Anisotropic Aerogel

T. Kunimatsu\*, T. Sato<sup>+</sup>, K. Izumina<sup>+</sup>, A. Matsubara<sup>+\*∇</sup>, Y. Sasaki<sup>\*∇</sup>, M. Kubota<sup>+</sup>, O. Ishikawa<sup>□</sup>, T. Mizusaki<sup>\*1)</sup>,  
Yu. M. Bunkov<sup>+△2)</sup>

<sup>+</sup>*Institute for Solid State Physics, The University of Tokyo, Chiba 277-8581, Japan*

\* *Department of Physics, Graduate School of Science, Kyoto University, Kyoto 606-8502, Japan*

□ *Graduate School of Science, Osaka City University, Osaka 558-8585, Japan*

∇ *Research Center for Low Temperature and Materials Sciences, Kyoto University, Kyoto 606-8502, Japan*

△ *MCBT, Institute Neel, CNRS, 38042, Grenoble, France*

Submitted 21 June 2007

We report on the orientation of the order parameter in the A-like and B-like phases of superfluid  $^3\text{He}$  immersed in uniaxially-compressed aerogel. By NMR methods we find that the orbital momentum of the A- and B-like phases is oriented along the deformation. In the A-like phase we observe a relatively narrow NMR line with an anomalously large negative frequency shift. We have succeeded in measuring the Leggett frequency in the A-like phase which shows the same energy gap suppression as in the B-like phase.

PACS: 67.57.-z

**1. Introduction.** Superfluid  $^3\text{He}$  has the most complex order parameter encompassing many degrees of freedom which can currently be successfully described by a comprehensive theory. Furthermore, many quantum phenomena observed in superfluid  $^3\text{He}$  can be used to test general concepts in other areas of physics, from non-conventional Cooper pairing, BEC, Bose condensation of spin waves [1] to cosmology [2, 3]. The influence of disorder on ordered states is one of the most interesting and ubiquitous problems in condensed matter physics. In superfluid  $^3\text{He}$  the disorder can be introduced by immersing the liquid in high porosity silica aerogel. It has been found that the disorder in the aerogel gives rise to significant changes in the superfluid phase diagram. Not only is the critical temperature suppressed, but there are also changes in the ground states of A-like and B-like phases as well as in the temperature and dynamics of the transition between them.

Of particular interest is the question of the influence of the local random anisotropy of the aerogel on the superfluid order of the  $^3\text{He}$  A-like phase. The orbital momentum part of the order parameter should be very sensitive to the local aerogel anisotropy. Short length-scale anisotropy can lead to a Larkin-Imry-Ma state [4]. The aerogel anisotropy on the scale larger than the textural healing length (  $10\ \mu\text{m}$  in the A phase and  $1\ \text{mm}$

in the B phase) leads to inhomogeneous broadening of NMR lines and creation and stabilization of textural and topological defects. Experimental evidence of topological defects contaminating in the B-like state in aerogel has been observed in Grenoble [5], where NMR signals were found to be superpositions of signals with different properties. Similar observations for the A-like phase are described in ref. [6]. The aerogel inhomogeneity can play a role of defects formation [2, 3] in the same way as dark matter fluctuations play a role for fluctuations of relic radiation [7]. It was thought that in bulk superfluid  $^3\text{He}$  the disorder and topological defects generated on passage through the transition can easily dissipate. However, some types of defects can survive in superfluid  $^3\text{He}$  even in the bulk [8]. In the superfluid in aerogel, topological defects can survive by attaching to some peculiarities of the aerogel structure. This provides an interesting example of a system with continuous symmetry in the presence of random anisotropy disorder. Recently it was found [9] that the response of the A-like phase to superfluid flow is highly anisotropic, revealing that texture and defects can be easily modified by flow.

Recently much interest has been paid to aerogel with a global anisotropy. It has been suggested that anisotropic aerogel might lead to new phases of superfluid  $^3\text{He}$  [10], in particular the “polar” state [11, 12]. However, the property of the superfluid most sensitive to the anisotropy of the aerogel is NOT the deformation of the superfluid state but rather the orientation of the

<sup>1)</sup> Current address: Toyota Physical and Chemical Research Institute, Nagakute, Aichi 480-1192, Japan

<sup>2)</sup> e-mail: yuriy.bunkov@grenoble.cnrs.fr

orbital momentum of Cooper pairs. In this article we present the first experimental observation of this orientational effect of the anisotropy in aerogel.

Global anisotropy can be imposed during the process of growth and drying [10]. We have introduced in this article the more direct method of anisotropic aerogel formation. We have used the axial deformation of isotropic aerogel by external force. We can explain the effect of axial deformation on the orientation of order parameter in superfluid  $^3\text{He}$  by consideration, suggested by Volovik [13, 14]. Let us consider the isotropic aerogel as a randomly distributed cylinders of radius  $R \ll \xi$  with the length of a cylinder and the distance between cylinders equal to  $l \gg R$ . The characteristic energy of each of a small cylindrical object with  $R \ll \xi$  is according to [15]:

$$k_F^2 R l \frac{\Delta^2}{T_c}. \quad (1)$$

The axial deformation of aerogel leads to the appearance of a regular arrangement of cylinders. If one squeezes the sample of length  $L$  by  $\Delta L$ , then the preferable orientation of the ensemble of cylinders will be of order of  $\lambda = \Delta L/L$  in the direction, perpendicular to the axis of deformation. This slightly non-random distribution of orientation of cylinders contributes to the energy density

$$\epsilon_{\text{regular}} = -\lambda \frac{k_F^2 R \Delta^2}{l^2 T_c} (\mathbf{L} \cdot \hat{\mathbf{z}})^2, \quad (2)$$

where  $\hat{\mathbf{z}}$  is the direction of the regular anisotropy axis caused by deformation and  $\mathbf{L}$  is the unit vector along the direction of the orbital momentum of Cooper pairs. This energy which orients the  $\mathbf{L}$ -vector along  $\hat{\mathbf{z}}$  must be compared with the orientational energy caused by dipole-dipole interaction,

$$\epsilon_{\text{dipole}} = -\lambda_D \frac{k_F^2 \Delta^2}{\xi_0 T_c} (\mathbf{L} \cdot \hat{\mathbf{d}})^2, \quad (3)$$

orienting the  $\mathbf{L}$ -vector along the magnetic vector  $\mathbf{d}$ , which in turn is perpendicular to the magnetic field. Since  $\lambda_D$  is about  $10^{-7}$  and  $R\xi_0/l^2$  is about 100, a very small deformation of aerogel  $\lambda$  can reorient  $\mathbf{L}$  along the direction of deformation.

Our experiments with superfluid  $^3\text{He}$  in aerogel under an axial deformation confirm that orbital momentum in the A- and B-like phases is indeed oriented along this deformation axis causing changes in the NMR signatures of both phases. NMR signals from the A-like phase display a large negative frequency shift, while those from the B-like phase remain close to the Larmor frequency,

consistent with the orientation of the orbital momentum along the magnetic field. We also observe broadening of the NMR line, probably arising from the effect of the inhomogeneity of the aerogel anisotropy on a length scale larger than the textural healing length. We were also able, for the first time, to observe the dependence of the A-B transition temperature on the NMR frequency shift. This effect may shed light on the mechanism of the A-B transition in aerogel.

**2. Experimental setup.** The aerogel sample used was of 98% porosity material, made by N. Mulders, in the form of a cylinder of diameter 5 mm and length 3 mm with the axis oriented along the external magnetic field direction. We expect that the aerogel was squeezed by about 3% and 2% along the axis at two sets of our experiment. We have placed the aerogel sample inside the cell of diameter 5.2 mm, made from Stycast 1266. At the process of closing the cell, we have pressed it by about 20% and then released the pressure. We can estimate, that the deformation, remaining after releasing the pressure, i.e. the plastic deformation, was of about 2% (see analysis below for comparison between two runs). We carried out two sets of experiments. In the first, there was no gap between the aerogel and top and bottom surfaces of the cell. On cooling the Stycast body contracts about 1% more than aerogel itself. Consequently, in the first set of experiments the aerogel sample had an additional deformation along the axis of about 1% more than as pre-deformed at room temperature. In the second set of experiments the aerogel was fitted loosely into the cell which had gaps between the aerogel and the cell, and thus with no additional deformation due to thermal contraction.

All the experiments described below were made at 29.3 bar pressure in a magnetic field of 290 gauss, corresponding to an NMR frequency of 940 kHz. The  $^3\text{He}$  in the aerogel cell was connected to the bulk  $^3\text{He}$  by a channel of 1 mm diameter. Thermometry was based on a melting curve thermometer placed outside of the cell. To avoid the formation of solid  $^3\text{He}$  on the surface of aerogel strands, we preplated the aerogel with layers of  $^4\text{He}$ . The cell was installed on a rotating nuclear demagnetization cryostat of ISSP, University of Tokyo, which allowed us to observe the influence of rotation on the observed NMR signals. To make the measurements we have used both conventional cw NMR spectroscopy and the Homogeneous Precessing Domain (HPD) method of NMR [16].

**3. Experimental results.** In the A-like phase we observe a relatively narrow NMR line with a large negative NMR frequency shift, shown in Fig.1. The NMR frequency in the A-like phase depends on the relative ori-

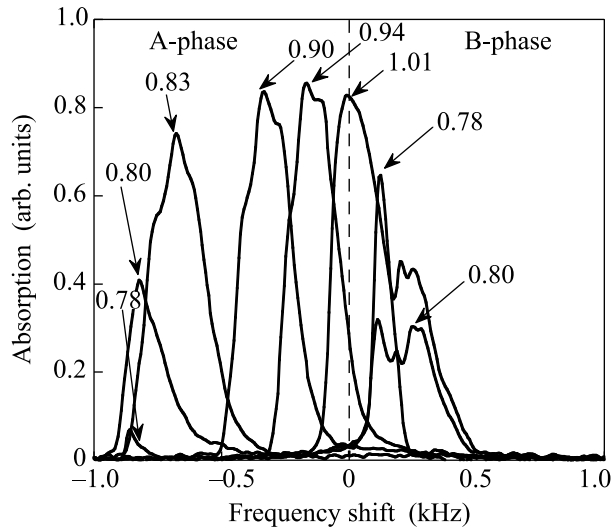


Fig.1. The cw NMR signals for various temperatures, labelled on each curve as  $T/T_c^a$ . Those signals with negative frequency shift are from the A-like phase and those with positive frequency shift from the B-like phase

entation of the orbital momentum  $\mathbf{L}$  and the spin vector  $\mathbf{d}$  according to [17]:

$$\omega^2 = \omega_l^2 + \Omega_A^2(1 - 2 \sin^2 \beta), \quad (4)$$

where  $\omega_l$  is the Larmor frequency,  $\Omega_A$  is the Leggett frequency in the A phase and  $\beta$  is the angle between  $\mathbf{L}$  and  $\mathbf{d}$ . In the applied magnetic field, the spin vector  $\mathbf{d}$  is oriented perpendicular to  $\mathbf{H}$ . The dipole-dipole energy orients  $\mathbf{L}$  along  $\mathbf{d}$ , which usually leads to the observed positive NMR frequency shift. Contrary to that, in our experiments we see a big negative frequency shift, which shows that  $\sin^2 \beta > 1/2$ . The quantitative analysis of frequency shift shows that  $\sin^2 \beta \simeq 1$ , as shown in Fig.4.

Below  $0.82 T_c^a$  (with  $T_c^a$  being the transition temperature of the A-like phase) a fraction of the superfluid A-like phase undergoes a transition to the B-like phase. NMR signals from the bulk B phase usually show a very broad distribution extending from the Larmor frequency to a large positive shift arising from the texture. In Fig.1 in contrast, we see a relatively narrow NMR line with a small positive shift, which is most naturally explained as arising from the orientation of the induced orbital momentum along the magnetic field. We can claim that this orientation of the orbital momenta in both phases is indeed the result of the orientational effect of the aerogel anisotropy. In Fig.2 we show the frequency shift for the peak of the NMR absorption signal for the A-like and B-like phases.

The shape of NMR spectrum is determined by the spatial distribution of  $\mathbf{L}$  and  $\mathbf{d}$  according to equation

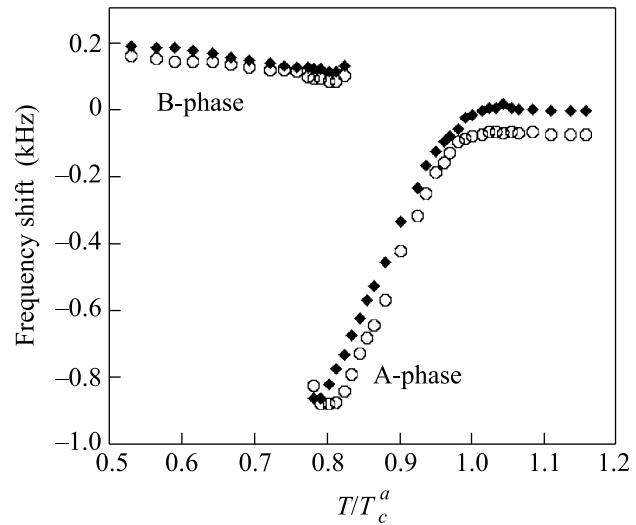


Fig.2. The frequency shift of the peak of NMR spectrum. Results for the first set of experiments ( $\bullet$ ) and for the second set ( $\diamond$ )

(4). Our estimations shows that in the first set of experiments the maximum frequency shift reaches the value corresponding to orientation of  $\mathbf{L}$  parallel to the magnetic field, and consequently, perpendicular to  $\mathbf{d}$ . If this is the case, the maximum frequency shift, shown in Fig.3 by solid circles, should be equal to  $-\Omega_A^2/2\omega$ . In order

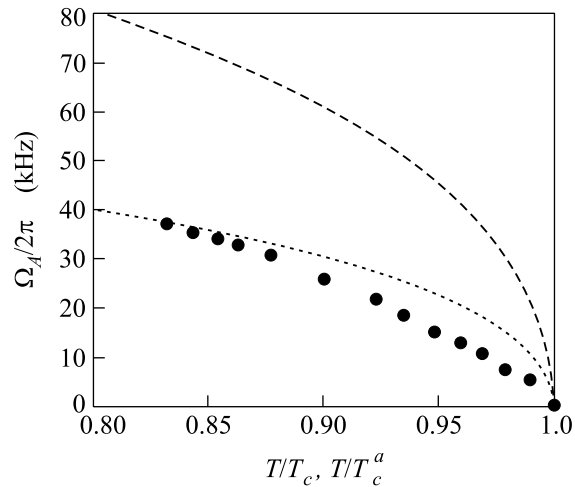


Fig.3. The values of  $\Omega_A^a$  calculated from the NMR shift for the first set of experiments ( $\bullet$ ). The dashed line shows the value of  $\Omega_A$  for bulk  $^3\text{He}$  against reduced temperature. The dotted line shows the corresponding 50% value of  $\Omega_A^a$  for bulk plotted as  $T$  over  $T_c^a$

to confirm this conclusion we need to estimate the magnitude of  $\Omega_A^a$  for aerogel, which has not been measured previously. In the case of isotropic scattering model [18] the ratio  $\Omega_B/\Omega_A$  for the aerogel should be the same as

for the bulk case. The value of  $\Omega_B^a$  in aerogel has been studied by various methods [19]. From these data we can estimate a 50% reduction of  $\Omega_A^a$  in aerogel at 29.3 bar, as shown in Fig.3 (dotted line). As can be clearly seen, at low temperatures the measured  $\Omega_A^a$  ( $\bullet$ ) approaches the estimated value. At higher temperatures the frequency shift becomes smaller than predicted by isotropic scattering. This can be explained by anisotropic scattering model [18].

We may suppose that the sample of aerogel before the global deformation is applied is not homogeneous. There are regions with local deformation which are oriented randomly. In a squeezed aerogel the local deformations are oriented mainly along the axis, but with some scattering. The additional pressure arising from the Stycast constraint, makes the orientation more parallel to the axis. We can characterize the shape of the  $^3\text{He}$ -A NMR spectrum in a local approximation. The difference in the distribution of  $\beta$  between the first and the second runs could be caused by the additional thermal contraction due to Stycast cell in the first run. Simple calculations shows, that the distribution of angles in Fig.4 can be explained by about 1% of random orientation in the aerogel before the deformation, additional 2% orientation along the axis at the second set of data, and additional 3% orientation in the first set of data.

We can confirm this picture by looking at the NMR data for the B-like phase. The textural healing length in the B-like phase is much greater than that in the A-like phase. Thus averaging over this longer scale makes the effective mean deviation of the random orientation very small. That is why the B-like phase shows nearly vertical orientation of the average  $\mathbf{L}$  in both cases. The small deviation from zero frequency shift can be explained by the well-known NMR shift due to spin waves, which are not taken into account in our local approximation.

Surprisingly we have found that the transition temperature from the A-like to B-like phase depends on the frequency shift in  $^3\text{He}$ -A. Previous studies have shown that the A-like and B-like phases can coexist over some range of temperatures [20–22]. We observed that on cooling, that part of the  $^3\text{He}$ -A phase with the largest frequency shift undergoes the transition first (see Fig.1). For those experiments without the Stycast constraint the effect is even more pronounced. It should be noted that in the second run the frequency shift of NMR spectrum ( $\circ$ ) starts to increase at some temperature even though  $\Omega_A^a$  should continuously increases as temperature decreasing (see Fig.2). The greater the angle of deviation of  $\mathbf{L}$  from the magnetic field direction, the smaller is the frequency shift and the lower the transition temperature (see Fig.2). It is a problem for the theory to explain the

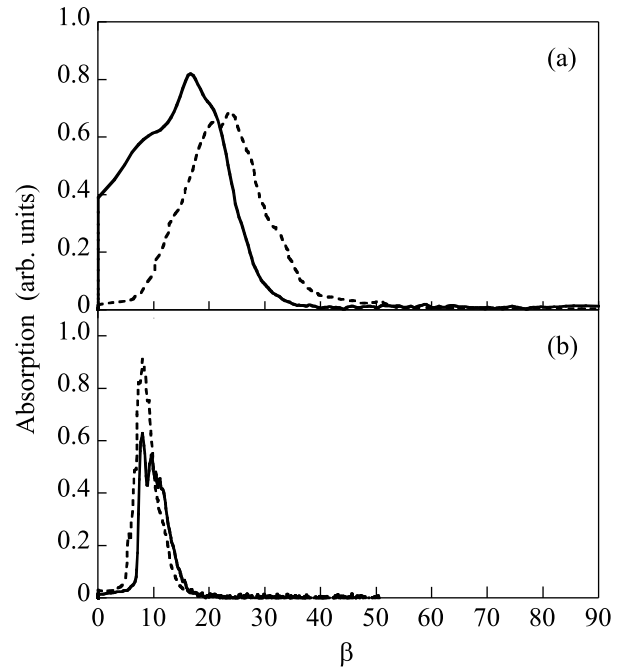


Fig.4. The spread of the NMR signal in the A-like (a) and B-like (b) phases plotted as function of the angle of deflection  $\mathbf{L}$  from the vertical in a local NMR approximation. The solid line shows the signal from the run with the Stycast constraint, and the dashed line shows the signal after the pressure release (see text)

dependence of the A-B transition temperature on the orientation of  $\mathbf{L}$ .

We have performed many different experiments under rotation. We have cooled through the transition under rotation, or simply rotated at constant temperature, or rotated with the simultaneous creation of an HPD. From these experiments we conclude that counterflow has negligible influence on the orientation effects on  $^3\text{He}$ -A in squeezed the aerogel. This is a direct consequence of aerogel orientation energy. The counterflow energy can be on an order of magnitude bigger than the dipole energy, but it is not enough for reorient the vector  $\mathbf{L}$  in a percent squeezed aerogel. In  $^3\text{He}$ -B the aerogel orientation energy is significantly smaller owing to the small value of orbital momentum, induced by magnetic field. We can see some influence of rotation in B-like phase when we cross  $T_c^a$  under rotation. In this case spin-waves modes are clearly seen in the B-like phase [23]. The effect of counterflow, observed in reference [24] can also be seen but with very small amplitude in deformed aerogel. In the A-like phase we observe the formation of a state with coherent precession of magnetization which will be discussed elsewhere.

**4. Discussion and conclusions.** To conclude, we have demonstrated for the first time that the global anisotropy of aerogel has a strong influence on the orientation of the orbital momentum in both the A-like and B-like phases. In both phases the orbital momentum orients itself along the direction of the squeezing. The resultant line broadening in the A-like phase is greater than that in B-like phase owing to the difference in the respective textural healing lengths.

We also shed new light on the problem of orientating effect of the aerogel surface. It has been found [19] that the free surface of aerogel orients  $\mathbf{L}$  in the B-like phase parallel to the surface. From our results this effect can be explained by the presence of a local deformation in the aerogel caused by the mechanical slicing of the sample. Such treatment can lead to a dense layer of aerogel near the surface.  $\mathbf{L}$  can then be oriented by this layer, rather than by the aerogel surface itself.

We are grateful to N. Mulders for providing the aerogel sample and to G. Pickett, J. Pollanen and G. Volovik for many discussions. The work was undertaken in the ISSP. The collaboration was supported by CNRS-JSPS project PRC- 88, the 21 century COE program and the KAKENHI program (grant 17071009). Yu. Bunkov is grateful for ISSP hospitality during this work.

- 
1. G. E. Volovik, cond-mat/0701180; Yu. M. Bunkov and G. E. Volovik, Phys. Rev. Lett. **98**, 265302 (2007).
  2. G. E. Volovik, *The Universe in a Helium Droplet*, Oxford Science Publications, Clarendon Press, Oxford 2003.
  3. C. Bäuerle, Yu. M. Bunkov, S. N. Fisher et al., Nature **382**, 332 (1996).
  4. G. E. Volovik, JETP Lett. **81**, 647 (2005).
  5. Yu. M. Bunkov et al., Physica B **329**, 305 (2003).
  6. V. V. Dmitriev et al., JETP Lett. **84**, 461 (2006).
  7. During of the fast cooling of the Universe, fluctuations in the baryonic matter density should have been smoothed out by plasma waves. However, the dark matter fluctuations remain and explain the current amplitude of the relic radiation, in the analogous way that inhomogeneity of local deformation in aerogel creates defects and texture in superfluid  $^3\text{He}$  (comment by Yu.M.B).
  8. C. B. Winkelmann et al., Phys. Rev. Lett. **96**, 205301 (2006).
  9. D. I. Bradley et al., Phys. Rev. Lett. **98**, 075302 (2007).
  10. J. Pollanen et al., J. Low Temp. Phys., Proc. QFS2006, cond-mat/0606784.
  11. K. Aoyama and R. Ikeda, Phys. Rev. B **73**, 060504 (2006).
  12. G. Barton and M.A. Moore, J. Low Temp. Phys. **21**, 489 (1975).
  13. G. E. Volovik, J. Low Temp. Phys., to be published, arXiv/0704.2484.
  14. G. E. Volovik, private communications.
  15. D. Rainer and M. Vuorio, J. Phys. C **10**, 3093 (1977).
  16. Yu. M. Bunkov, *Spin Supercurrent and Novel Properties of NMR in  $^3\text{He}$* , in *Progr. in Low Temp. Physics* **14**, 69, Ed. W. Halperin, Elsevier, 1995.
  17. Yu. M. Bunkov and G. E. Volovik, Europhys. Lett. **21**, 837 (1993).
  18. R. Hanninen and E. V. Thuneberg, Phys. Rev. B **67**, 214507 (2003).
  19. V. V. Dmitriev et al., AIP Conf. Proc. **850**, 229 (2006).
  20. V. V. Dmitriev et al., Physica B **329-333**, 320 (2003).
  21. C. L. Vicente et al., Phys. Rev. B **72**, 094519 (2005).
  22. J. E. Baumgardner, Phys. Rev. Lett. **93**, 055301 (2004).
  23. T. Kunimatsu et al., J. Low Temp. Phys., Proc. QFS2006, J. Low Temp. Phys., submitted.
  24. M. Yamashita et al., Phys. Rev. Lett. **94**, 075301 (2005).